Advances in Geo-Energy Research

Vol. 6, No. 5, p. 415-425, 2022

Original article

Hydrocarbon dynamic field division and its relevance to oil and gas exploration for Paleogene reservoir in Lufeng Depression

Kuiyou Ma[1,2], Hong Pang[1,2]*, Lili Zhang[3], Shengmin Huang[1,2], Xungang Huo[1,2], Junqing Chen[4]

[1]*State Key Laboratory of Petroleum Resources and Prospecting, China University of Petroleum, Beijing 102249, P. R. China*

[2]*College of Geosciences, China University of Petroleum, Beijing 102249, P. R. China*

[3]*Shenzhen Branch of China National Offshore Oil Corporation (CNOOC) Limited, Shenzhen 518054, P. R. China*

[4]*College of Sciences, China University of Petroleum, Beijing 102249, P. R. China*

Keywords:
Lufeng Depression
Paleogene
hydrocarbon dynamic field
oil and gas exploration

Cited as:
Ma, K., Pang, H., Zhang, L., Huang, S., Huo, X., Chen, J. Hydrocarbon dynamic field division and its relevance to oil and gas exploration for Paleogene reservoir in Lufeng Depression. Advances in Geo-Energy Research, 2022, 6(5): 415-425.
https://doi.org/10.46690/ager.2022.05.06

Abstract:
Significant breakthroughs have been achieved in the exploration of Paleogene reservoirs in the Lufeng Depression. However, as drilling depth is becoming greater, the discovered oil and gas reservoirs show signs of transition from conventional to unconventional accumulations, and the identification of conventional and unconventional reservoir boundaries is of particular significance. Herein, the hydrocarbon dynamic field boundaries in the Lufeng Depression are comprehensively identified by the geological drilling result method, the sandstone pore throat radius critical value discrimination method and the dry layer drilling rate variation method; then, the hydrocarbon dynamic field is divided and the characteristics and differences of hydrocarbon accumulations in each hydrocarbon dynamic field are compared. The results show that the buoyancy-driven hydrocarbon accumulation depth in the Lufeng Depression is between 3,500-4,000 m, and the hydrocarbon accumulation depth limit is about 5,800 m. The focus of research on Paleogene oil and gas exploration in the Lufeng Depression should be placed on conventional oil and gas reservoirs in the free dynamic field and tight oil reservoirs in the reformed dynamic field. As for the Enping Formation and Upper Wenchang Formation, efforts should concentrate on conventional oil and gas reservoir exploration, and the tight reservoir of Lower Wenchang Formation should be explored in the high fracture density area in C-4 and C-8 well blocks and the west of C-8 well block of the Lufeng 13 sag. The research results of this paper are of great value in further increasing oil and gas production and the explorarion of reservoirs in the Lufeng Depression.

1. Introduction

There are great prospects in hydrocarbon resource exploration in the Lufeng Depression within Zhu I depression in the Pearl River Mouth Basin (Tian et al., 2019). Recently, a series of breakthroughs were made in the exploration of deep fields, which are mainly in Paleogene reservoirs of the Pearl River Mouth Basin. Compared with shallow-buried reservoirs, Paleogene reservoirs have a significant advantage of "near-source accumulation". Although many oil-bearing reservoirs have been drilled in Paleogene reservoirs, their oil and gas productivity has been very poor, causing the poor success rate of commercial exploration in Paleogene reservoirs. This is mainly due to the co-existence of conventional and unconventional oil and gas in Paleogene reservoirs as a result of a complex hydrocarbon accumulation process. There are huge differences in the accumulation elements and processes between unconventional and conventional oil and gas (Karlsen and Skeie, 2006; Esmaili and Mohaghegh, 2016). Both can coexist in petroliferous basins, forming resource sequences

Yandy Scientific Press

*Corresponding author.
E-mail address: mky7201128@126.com (K. Ma); panghong19820107@126.com (H. Pang); zhanglili@cnooc.com.cn (L. Zhang); t13051070779@126.com (S. Huang); huo2020210115@126.com (X. Huo); cjq7745@163.com (J. Chen).

Received April 30, 2022; revised May 20, 2022; accepted June 3, 2022; available online June 8, 2022.

from shallow to deep reservoir (Magoon and Dow, 1994; Shi et al., 2005; Wang et al., 2015). On land, there are superior implementation conditions for horizontal well drilling technologies and reservoir reconstruction technologies, which can enable the exploration and development of conventional and unconventional oil and gas at the same time (Wang et al., 2017; Yuan et al., 2018). However, it is difficult to apply complex horizontal well drilling and reservoir reconstruction technologies in the Lufeng Depression, which is distributed in a marine area (Almedallah et al., 2021). Therefore, it is of great importance for oil and gas exploration in this area to accurately identify the depth boundary between conventional and unconventional reservoirs and further find a suitable resource distribution field for offshore oil and gas exploration and development.

Smith and Bustin (2000) approximately predicted the distribution field of unconventional oil and gas by summarizing the distribution characteristics and accumulation elements for unconventional oil and gas in the basin, which could roughly delineate the boundary between conventional and unconventional oil and gas. Jia et al. (2021) obtained the reservoir physical property boundary between conventional and unconventional oil and gas by analyzing the critical intermolecular force of oil and gas self-sealing state. Pang et al. (2021a) proposed a set of methods to analyze the boundary between conventional and unconventional oil and gas resources, including the numerical simulation method, geological drilling method, dry layer development frequency method and other methods, and put forward a series of related concepts. In addition, they defined the conventional and unconventional oil and gas fields as different hydrocarbon dynamic fields (HDFs) and defined the boundary of different HDFs as the hydrocarbon dynamic field boundary (HDFB). They further confirmed that different HDFs have different hydrocarbon accumulation characteristics and occurrence mechanisms.

It still remains unknown how to divide the HDFB and hydrocarbon dynamic field (HDF) in Paleogene reservoirs in the Lufeng Depression, what the differences are in oil and gas accumulation features in each HDF, and what value the exploration work on Lufeng depression may have when considering the research results of HDF. To answer these scientific questions, the following studies are carried out in this paper. Firstly, the concepts of HDF are introduced and the classification method of HDF is described. Secondly, utilizing the seismic data, reservoir physical data, high-pressure mercury injection data, logging interpretation data and imaging logging data, the HDFB and its distribution characteristics of Paleogene reservoirs in the Lufeng Depression are identified. Then, the key difference characteristics of oil and gas accumulations in each HDF of Paleogene reservoirs in the Lufeng Depression are summarized. Finally, based on the research results of the above three parts, some suggestions for further oil and gas exploration in the Lufeng Depression are given. Our findings are of considerable value in further increasing production and reservoir exploration in the Lufeng Depression.

2. Geological setting

The Lufeng Depression is located in the north of the Zhu I depression in the Pearl River Mouth Basin, South China Sea (Fig. 1(a)). Oil and gas accumulations mainly concentrate in the southern part of Lufeng Depression, including Lufeng 13 sag (LF13s), Lufeng 15 sag (LF15s), Lufeng 7 sag (LF7s) and their southern area (Wang et al., 2019). The tectonic evolution of Lufeng Depression is divided into two stages: Rifting stage (66.0-33.9 Ma) and thermal subsidence stage (33.9-0.0 Ma). During the rifting stage, the Lufeng Depression experienced Zhu-Qiong tectonic movement and South China Sea tectonic movement with intense tectonic intensity (Fig. 1(c)). Meanwhile, in the thermal subsidence stage, the Lufeng Depression experienced Baiyun tectonic movement and Dongsha tectonic movement with weakened tectonic intensity (Ge et al., 2020) (Fig. 1(c)). The whole Cenozoic Formation was developed within most area of the Pearl River Mouth Basin, including Paleogene Shenhu Formation, Wenchang Formation (WC), Enping Formation (EP) and Zhuhai Formation (ZH), Neogene Zhujiang Formation, Hanjiang Formation, Yuehai Formation and Wanshan Formation, and Quaternary Formation (Wu et al., 2022; Xie et al., 2022) (Fig. 1(c)). Among them, Paleogene WC and EP are the target formations in this study. EP can subdivided into four members, which include, from top to bottom, EP first member (EP_1) to EP fourth member (EP_4) (Niu et al., 2019). Among them, EP_1 and EP_2 are known as the Upper Enping Formation (EP_{1+2}), and EP_3 and EP_4 are known as the Lower Enping Formation (EP_{3+4}). WC can sub-divided into six members, which include, from top to bottom, WC first member (WC_1) to WC sixth member (WC_6). Among them, WC_1 to WC_3 are known as the Upper Wenchang Formation (WC_{1+2+3}), and WC_4 to WC_6 are known as the Lower Wenchang Formation (WC_{4+5+6}).

The existing research results for source rocks show that the mudstone of WC is an important source rock in the Lufeng Depression (Wang et al., 2019). From WC_{4+5+6} to EP_{1+2}, the shale content of reservoir gradually decreases (Fig. 1(c)). The sedimentation environment of WC_{4+5+6} is mainly lacustrine facies, and WC_{4+5+6} also develops limit delta facies in the south of the Lufeng Depression. The mudstone of WC_{4+5+6} is an excellent source rock and regional caprock for the Lufeng Depression (Wang and Sun, 1994). In terms of lithologic composition, WC_{1+2+3} and EP are mainly filled by interbedded sand and mudstone, which leads to the situation that WC_{1+2+3} and EP have a good reserve condition and a poor selling condition for oil and gas (Zhang et al., 2003). The drill-stem testing (DST) measured formation pressure data of key well sets in the Lufeng Depression show that normal pressure is dominant in the depression, and only a certain weak overpressure phenomenon occurs in WC (Fig. 1(d)). The plane distribution of the discovered oil and gas reservoirs in Paleogene reservoirs in the Lufeng Depression is relatively limited, which are mainly in the interior and southeast of LF13s and southern of LF7s (Fig. 1(a)). Spatially, oil and gas are mainly accumulated in the EP reservoir near the B-1 well block in LF13s, which is also a structural reservoir. In the C-8 well block, oil and gas are mainly distributed in

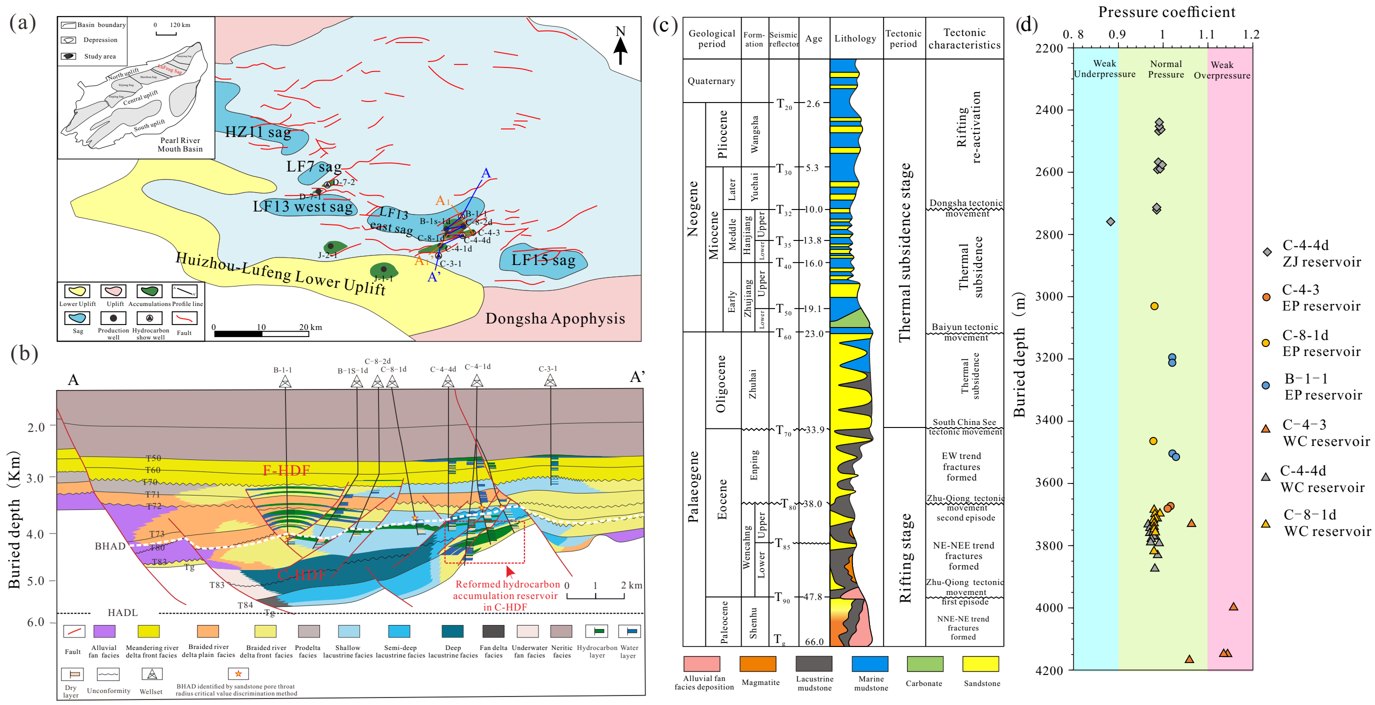

Fig. 1. (a) Geographical location map and structural division map of Lufeng Depression; (b) Key oil and gas accumulation profile of Lufeng Depression (the profile line is A-A' in Fig. 1(a)) and division result of HDF in Lufeng Depression (the profile line is A-A' in Fig. 1(a), the sources of star markings is from Fig. 3); (c) Histogram of stratigraphic lithology and tectonic evolution characteristics of Lufeng Depression; (d) Statistical map of DST measured formation pressure in Lufeng Depression.

WC_{1+2+3}, which also belong to structural reservoirs. In the C-4 well block that is located in the southeast of LF13s, a few oil and gas are distributed in EP_{3+4}, which belongs to lithologic reservoirs, while most of the oil and gas are mainly distributed in WC_{4+5+6}, which belongs to lithologic pinchout reservoirs. In addition, the oil and gas are mainly accumulated in the EP in the D-1 well block in the south of LF7s (Fig. 1(b)).

3. Method

3.1 Related concepts of hydrocarbon dynamic field

There is a huge difference in the distribution characteristics and controlling elements between unconventional and conventional hydrocarbon accumulations (Pang et al., 2021b). In shallow layers of petroliferous basins, oil and gas accumulations are mainly formed by buoyancy with normal density differentiation (Shanley et al., 2004). However, when the burial depth reaches a certain threshold, buoyancy is no longer the main driving force for hydrocarbon accumulation. Oil and gas will form tight oil and gas with abnormal density differentiation or remain in the source rock to form shale oil and gas (Zou et al., 2013). Therefore, there is an HDFB in petroliferous basins where buoyancy will not play a dominant role in oil and gas accumulation, which is called the buoyancy-driven hydrocarbon accumulation depth (BHAD) (Pang et al., 2021b). In addition, as the burial depth further increases, the physical properties of sandstone reservoirs gradually change and eventually approach the physical properties of mudstone at a certain depth value (Wang et al., 2020). Eventually, there is hardly any difference in the physical properties of the reservoir and the physical properties, which are extremely poor. Moreover, the probability of drilling a dry layer will approach 100% and there will be little likelihood for oil and gas accumulation (Pang et al., 2022). Therefore, the buried depth condition at which the pore throat radius of sandstone reservoir is equal to that of mudstone is taken as another HDFB, which is called the hydrocarbon accumulation depth limit (HADL) (Pang et al., 2021a). The reservoir areas above BHAD and between BHAD and HADL have different hydrocarbon accumulation dynamics and are called free hydrocarbon dynamic field (F-HDF) and confined hydrocarbon dynamic field (C-HDF), respectively (Pang et al., 2021a). In F-HDF, oil and gas accumulate in low-energy traps under buoyancy. The main types of oil and gas reservoirs are anticlinal reservoirs, lithologic reservoirs, fault reservoirs, stratigraphic oil and gas reservoirs, and hydrodynamic reservoirs. In C-HDF, oil and gas mainly form tight reservoirs at the bottom of the syncline or shale reservoirs within the source rocks. Nevertheless, C-HDF is not completely filled by tight reservoirs. In C-HDF, there are some local high-porosity and high-permeability reservoir areas formed by late fracture reconstruction, denudation reconstruction or dissolution reconstruction, which are called "sweet spots" and are important targets for unconventional oil and gas exploration. In the study of hydrocarbon accumulation dynamics, this reservoir area is also known as the "reformed hydrocarbon accumulation reservoir" (Pang et al., 2021a). It can be divided into three types: Fault-modified reservoir, dissolution modified reservoir and fault-dissolution modified reservoir. The reservoir area below the HADL is hardly capable of hydrocarbon accumulation and is called bound hydrocarbon dynamic field (B-HDF) (Pang et al., 2021a).

3.2 Method of HDFB identification

3.2.1 BHAD

In order to identify the BHAD, the geological drilling result method and the sandstone pore throat radius critical value discrimination method can be used (Pang et al., 2021a). Above BHAD, oil and gas usually present a normal oil-water contact relationship, while below BHAD, the oil-water contact relationship will become complicated and the phenomenon of "oil-water inversion" will occur in most cases. Therefore, BHAD can be identified based on the oil-water contact relationship, which is called geological drilling result method (Pang et al., 2022). In addition, the BHAD is also the boundary condition, such that buoyancy will not be the primary force in oil and gas accumulation. Thus, the physical condition of reservoir at the BHAD can be analyzed by using the force status of oil and gas in the reservoir, and then the physical condition can be used to identify BHAD (Guo et al., 2017; Pang et al., 2022). The physical simulation experiments and numerical analysis show that the reservoir's physical properties corresponding to BHAD are affected by the pore throat radius, oil and gas density, interfacial tension between oil and water, and wettability angle between the oil and gas and minerals (Guo et al., 2017; Pang et al., 2022). Among them, the pore throat radius of sandstone is the most important factor for the critical value of BHAD (Guo et al., 2017). Thus, BHAD can be identified by discriminating the critical value of sandstone pore throat radius, which is subsequently called sandstone pore throat radius critical value discrimination method.

3.2.2 HADL

In terms of HADL identification, the dry layer drilling rate variation method can be utilized (Pang et al., 2022). HADL is the critical geological condition for hydrocarbon accumulation. Theoretically, when the bound water saturation of a reservoir reaches 100%, there is no space for oil and gas to accumulate in the reservoir. Under this condition, the dry layer drilling rate will also reach 100%, which also means that the physical properties of the reservoir are no longer suitable for hydrocarbon accumulation. Therefore, the statistical relationship between reservoir physical properties and dry layer drilling rate can be used to determine the physical properties corresponding to HADL.

4. Results

4.1 HDFB identification

4.1.1 BHAD identification

In order to clarify the oil-water contact relationship of discovered oil and gas accumulations in the Paleogene reservoir, the profile map is drawn that can display most Paleogene oil and gas accumulations (Fig. 1(b)). Such accumulations above 3,550 m all exhibit the normal oil-water contact relationship in the Lufeng Depression. With the increase of buried depth, the number of drilled dry layers gradually increases, and the oil-water contact relationship becomes complex (Fig. 1(b)). The buried depth where abnormal oil-water contact relationship begins to show is taken as the critical value for BHAD identification. BHAD in the Lufeng Depression corresponds to buried depth distribution between 3,550 and 4,000 m, and it is deeper in the north than in the south (Fig. 1(b)).

Moreover, another method, the sandstone pore throat radius critical value discrimination method is used to further identify the BHAD. Based on the physical simulation experiment and numerical simulation method of homogeneous sandstone, Liu (2018) confirmed that the pore throat radius of sandstone corresponding to BHAD in Nanpu sag of Bohai Bay Basin is between 0.12 and 0.38 μm, with a mean of 0.28 μm. Since the Bohai Bay Basin and the Pearl River Mouth Basin are rift basins, the difference between them in geothermal gradient is small, and their sedimentary systems are similar, therefore the research result of Bohai Bay Basin is used to identify the BHAD in the Pearl River Mouth Basin, taking 0.28 μm sandstone pore throat radius as the critical value for BHAD identification (Liu, 2018). Since it is difficult to obtain the pore throat radius data of the reservoir, the numerical relationship between the porosity and pore throat radius of sandstone reservoir is established based on high-pressure mercury injection data and thin-section data (Fig. 2). According to the numerical relationship, the porosity of sandstone corresponding to the BHAD is calculated, and it is 10.96%. Due to the heterogeneity of reservoirs, the porosity of sandstone reservoirs at different burial depths is not a constant value, and it is difficult to find the critical physical condition corresponding to the BHAD (Tan et al., 2017). In this paper, the average porosity of each buried depth sandstone reservoir is used to describe the pore characteristics. The average porosity evolution map of key well sets is established, and the BHAD is further identified (Fig. 3). The results show that the buried depth corresponding to BHAD in the northern Lufeng Depression is about 4,075 m, and it is about 3,490 m in the south of the depression. This is slightly shallower than the BHAD identified by the geological drilling result method, but they still have high consistency (Fig. 1(b)).

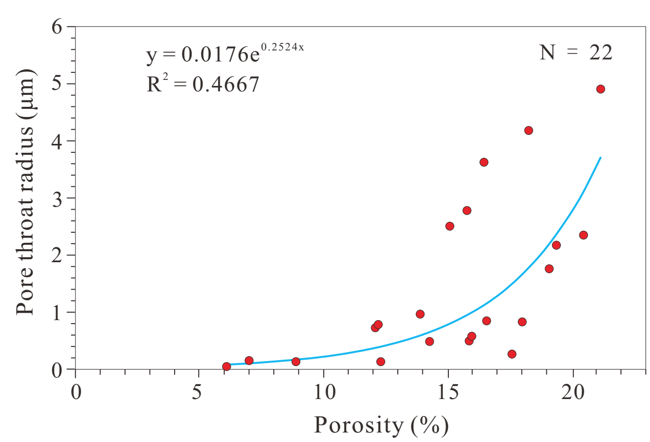

Fig. 2. Intersection diagram of reservoir porosity and pore throat radius in Lufeng Depression.

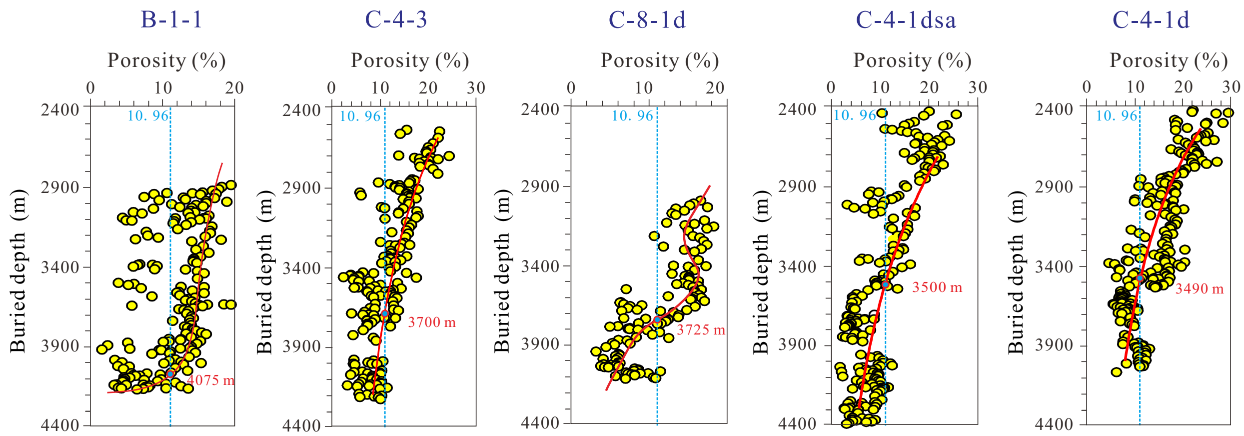

Fig. 3. Porosity evolution map of key well sets in Lufeng Depression (the profile line is A_1-A_1' in Fig. 1(a), BHAD of each well set has been marked by a star in Fig. 2).

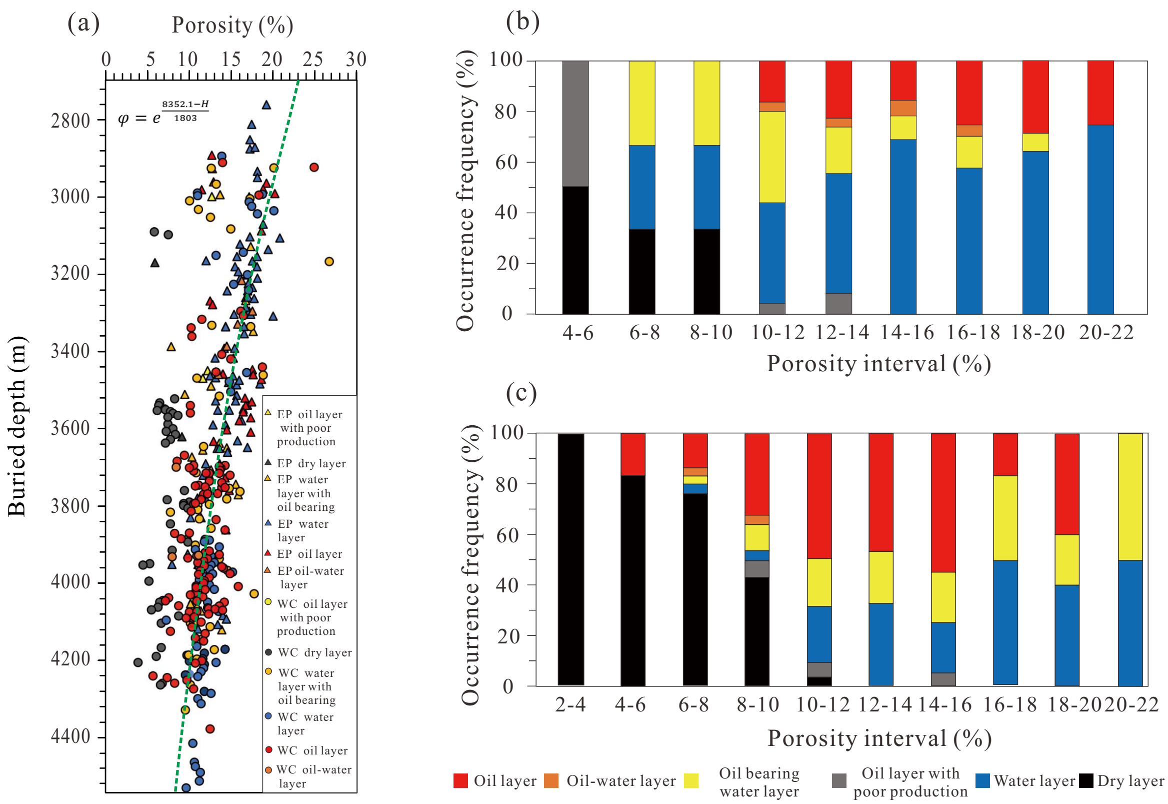

Fig. 4. (a) Reservoir porosity evolution map of EP and WC in Lufeng Depression; (b) Relationship map between reservoir porosity and dry layer drilling frequency in EP; (c) Relationship map between reservoir porosity and dry layer drilling frequency in WC.

4.1.2 HADL identification

Under BHAD, with the increase of burial depth, the physical properties of sandstone reservoirs of EP and WC are further reduced and the dry layer drilling ratio increases rapidly (Fig. 4). In a shallow-buried EP reservoir, a dry layer begins to be drilled when the reservoir porosity is equal to 10%. In addition, with the decrease of physical properties, the proportion of drilled dry layers increases in the reservoir, while the proportion of dry layers drilled is not up to 100% (Fig. 4(b)). In a WC reservoir with a buried depth greater than EP, a dry layer begins to be drilled when the reservoir porosity is equal to 12%. The proportion of drilled dry layers reaches 100% when the porosity is equal to 4% (Fig. 4(c)). Compared with EP, the physical properties of dry layers begin to appear higher in WC, and the increment for the ratio of drilled dry layers is larger with the decrease of reservoir physical properties (Figs. 4(b) and (c)). This may be due to the higher shale content in WC reservoirs deposited in extensive lacustrine facies (Fig. 1(c)). Overall, the EP reservoir has not reached the HADL, while part of the WC reservoir with low physical properties is over the HADL. The critical physical condition of HADL is that the porosity is equal to 4%. Based on the porosity data of EP and WC reservoirs, a numerical model of porosity evolution is established (Fig. 4(a)). The evolution trend of reservoir porosity in EP and WC is consistent (Fig. 4(a)), which presents a relatively regular exponential relationship (Eq. (1)):

$$\varphi = e^{\frac{8352.1-H}{1803}} \tag{1}$$

where φ represents reservoir porosity, %; H represents buried depth, m.

Combined with the porosity critical condition corresponding to HADL and the numerical model of porosity evolution, it can be concluded that the burial depth corresponding to HADL is about 5,800 m in the Lufeng Depression.

4.2 HDFs division and key period

4.2.1 HDFs division

Based on the distribution characteristics of BHAD and HADL, the Paleogene reservoir can be divided into two HDFs, which are F-HDF and C-HDF, respectively. The F-HDF in the Lufeng Depression is mainly distributed in the WC_{1+2+3} and EP reservoirs, and the types of oil and gas reservoirs are primarily anticline and fault reservoirs (Fig. 1(b)). The C-HDF is mainly distributed in the deeply buried reservoir of WC. In the sags of Lufeng Depression, there are few faults in C-HDF, which also means that the reforming effect of C-HDF reservoir by faults is weak and the types of oil and gas reservoirs are mainly tight oil reservoirs in the sags (Fig. 1(b)). In the C-4-1d well block outside of the LF13s, the C-HDF is strongly reformed by faults, and typical reformed oil and gas reservoirs are developed, most of which are lithologic oil and gas reservoirs (Fig. 1(b)). The detailed characteristics of this reservoir are described in Section 4.3.

The maximum burial depth of sedimentary formation in the Lufeng Depression is about 5,600 m (Fig. 1(b)). There is almost no sedimentary formation distributed below the HADL in the Lufeng Depression. The burial depth corresponding to the BHAD in the Lufeng Depression is between that of EP and WC of the Paleogene reservoir. For oil and gas exploration, it is important to clarify the plane distribution characteristics of BHAD in Paleogene EP and WC reservoirs. The porosity plane distribution maps of sandstone reservoirs in EP_{1+2}, EP_{3+4}, WC_{1+2+3} and WC_{4+5+6} are drawn. According to these maps, the plane distribution characteristics of BHAD are analyzed by taking the sandstone porosity of 10.96% as the physical property critical value corresponding to BHAD. The EP_{1+2} is above the BHAD, since it is shallow-buried (Fig. 5). Part of the EP_{3+4} and WC_{1+2+3} reservoirs exceed the BHAD, but the distribution of these reservoirs is relatively limited, only covering the middle and north of LF13s (Fig. 5). Most of the WC_{4+5+6} reservoirs are under the BHAD, including most areas of LF15s and LF13s (Fig. 5).

4.2.2 Key period of HDF evolution

The key period of HDF evolution is obtained based on the division result of BHAD in the Lufeng Depression and the evolution map of burial history and thermal history of B-1 well block located in LF13s and C-4 well block located in the southern edge of LF13s (Fig. 6). At the inner part and the edge of the depression, the depths of 4,000 m and 3,500 m, respectively, are used as the geological limits of BHAD. In the inner depression, the deep part of WC_{4+5+6} began to exceed the BHAD at 13 Ma and completely exceeded the BHAD at 3 Ma. In addition, most of the WC_{1+2+3} is also below BHAD nowadays. At the edge of the depression, the deep of WC_{4+5+6} began to exceed the BHAD at about 10.5 Ma, and completely entered the BHAD about at 4.9 Ma. At present, the whole WC and a small part of EP are below the BHAD. In conclusion, the period for deep WC_{4+5+6} reservoir that began to exceed the BHAD was at about 13-10.5 Ma, and the period for deep WC_{4+5+6} reservoir that completely exceeded the BHAD was at about 4.9-3 Ma. At present, almost the whole WC reservoir is below the BHAD, and only a limited part of the EP reservoir is below the BHAD.

4.3 Characteristics of oil and gas accumulations in individual HDFs

4.3.1 Characteristics of oil and gas accumulations in F-HDF

The EP oil and gas accumulation drilled by the B-1-1 well is located in the inner part of LF13s (Figs. 1(a) and (b)) and is distributed in F-HDF. The type of this accumulation is anticline reservoir with clear and normal oil-water contact relationship. Moreover, oil and gas accumulate at the high part of the anticline and are capped by muddy cap rocks (Fig. 7(a)). Pang et al. (2021a; 2021b; 2022) extensively studied the physical property of tight oil and gas reservoir in many basins in China and proposed that 10% $\pm$ 2% porosity and 1 mD permeability is the critical value corresponding to BHAD. It could be seen that the porosity of a reservoir corresponding to BHAD in each basin considerably varies and is easily affected by the actual geological conditions, while permeability corresponding to BHAD in each basin is almost stable at about 1 mD with a small variation range. Based on the research results of this paper, 10.96% porosity and 1 mD permeability are taken as the reservoir physical properties corresponding to BHAD in Lufeng Depression. The porosity and permeability of B-1-1 EP reservoir range from 11% to 18% and from 1 to 1000 mD, and this physical property value is higher than that corresponding to BHAD (Fig. 7(b)). This also suggests that the EP oil and gas reservoirs drilled by B-1-1 well are distributed in F-HDF. In addition, the migration and accumulation process of these reservoirs have typical conventional accumulations characteristics: The source rock is far away from the reservoir and there is an obvious migration path from source rock to reservoir along the faults and sandstones (Fig. 7(a)).

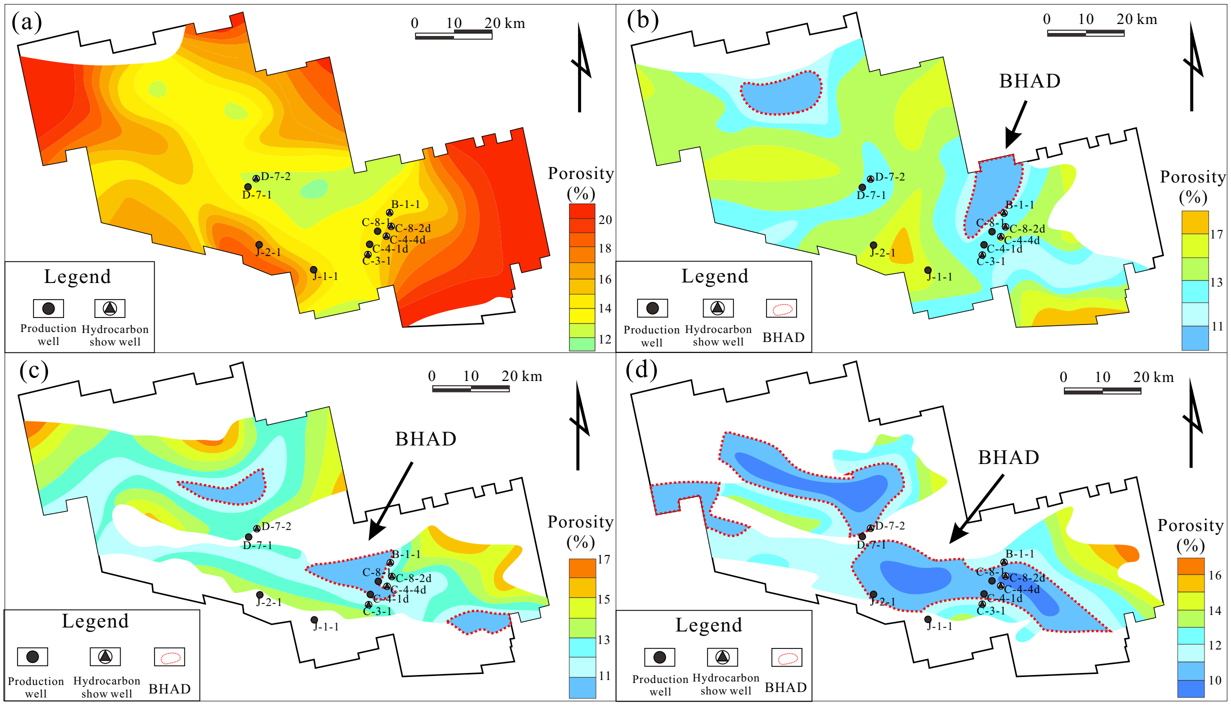

Fig. 5. (a) Plane distribution of sandstone porosity and BHAD in EP_{1+2} reservoir; (b) The plane distribution of sandstone porosity and BHAD in EP_{3+4} reservoir; (c) The plane distribution of sandstone porosity and BHAD in WC_{1+2+3} reservoir; (d) The plane distribution of sandstone porosity and BHAD in WC_{4+5+6} reservoir.

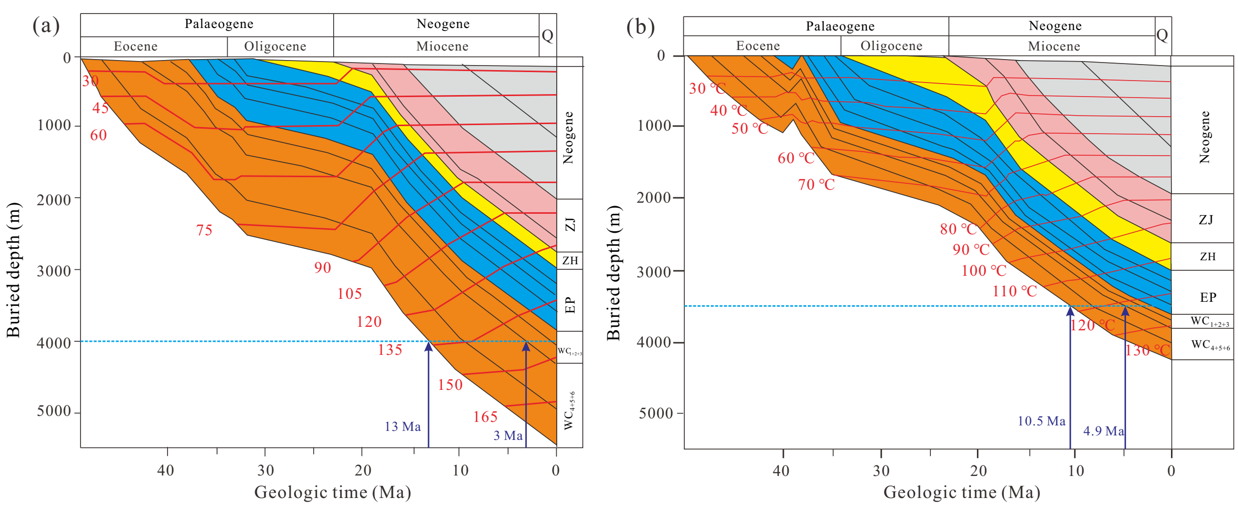

Fig. 6. (a) Map of the burial history and thermal history of B-1 well block in the inner part of Lufeng Depression; (b) Map of the burial history and thermal history of C-4 well block at the edge of Lufeng Depression.

4.3.2 Characteristics of oil and gas accumulations in C-HDF

The WC_{1+2+3} oil and gas accumulation drilled by the B-1s-1d well is also located in the inner part of LF13s, which is distributed in C-HDF (Figs. 1(a) and (b)). This oil and gas accumulation is closely adjacent to the WC source rock and accumulates at the bottom of the syncline (Fig. 8). According to the intersection diagram for measured porosity and permeability, it can be found that the porosity and permeability of the reservoir in this oil and gas accumulation ranges from 2% to 11% and from 0.01 to 1 mD, respectively, which suggests that the physical property for reserve condition is extremely poor (Fig. 8). Moreover, according to the well logging interpretation data of B-1s-1d (Fig. 8(c)), the WC_{1+2+3} oil and gas accumulation consist of dominantly tight oil layers without production (38 m of that drilled by B-1s-1d), and the WC_{1+2+3} has very high sandy content with a poor sealing condition, which is composed by a thin mudstone layer whose thickness is less than 1 m (Fig. 8(c)). Lastly, the actual test data show that oil and gas accumulation has no prospect for investment due to very low productivity. Based on the above

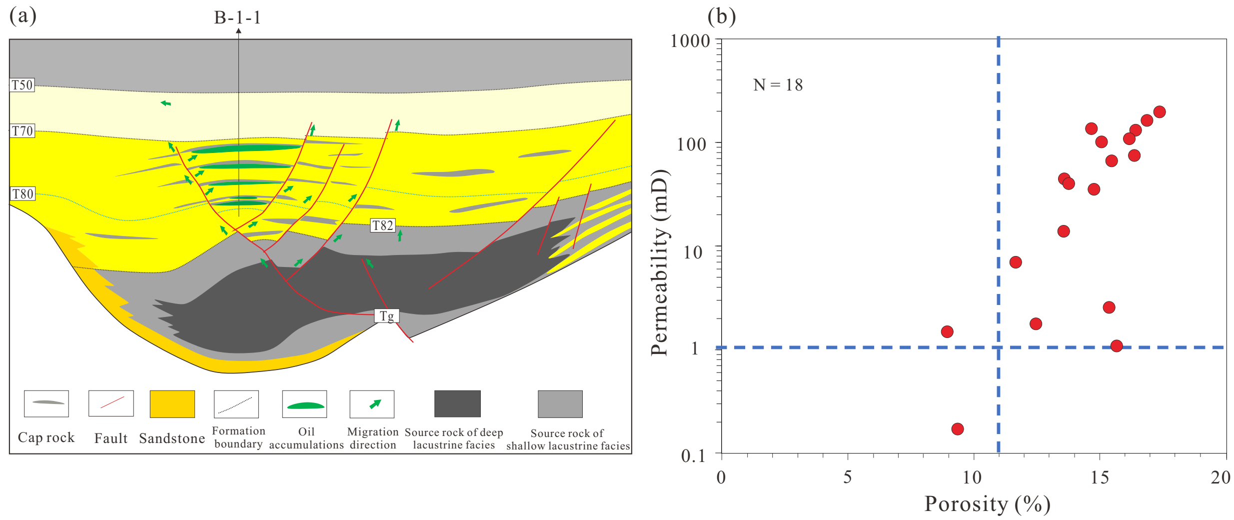

Fig. 7. (a) Forming model diagram for EP oil and gas accumulations drilled by B-1-1 well; (b) Intersection diagram of reservoir porosity and permeability of B-1-1 EP reservoir.

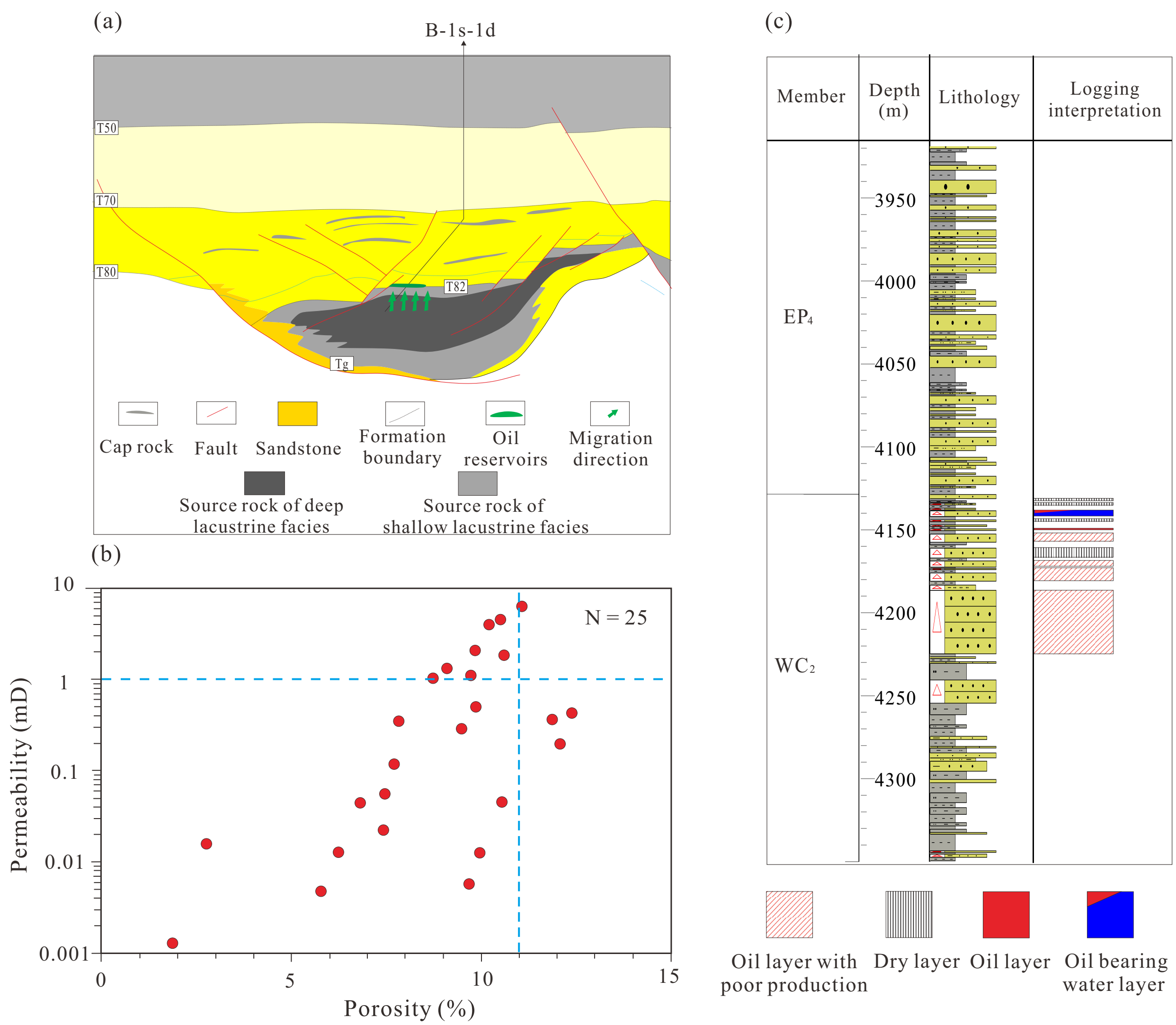

Fig. 8. (a) Forming model diagram for WC_{1+2+3} oil and gas accumulations drilled by B-1s-1d well; (b) Intersection diagram of reservoir porosity and permeability of B-1s-1d WC_{1+2+3} reservoir; (c) Logging interpretation histogram of B-1s-1d well.

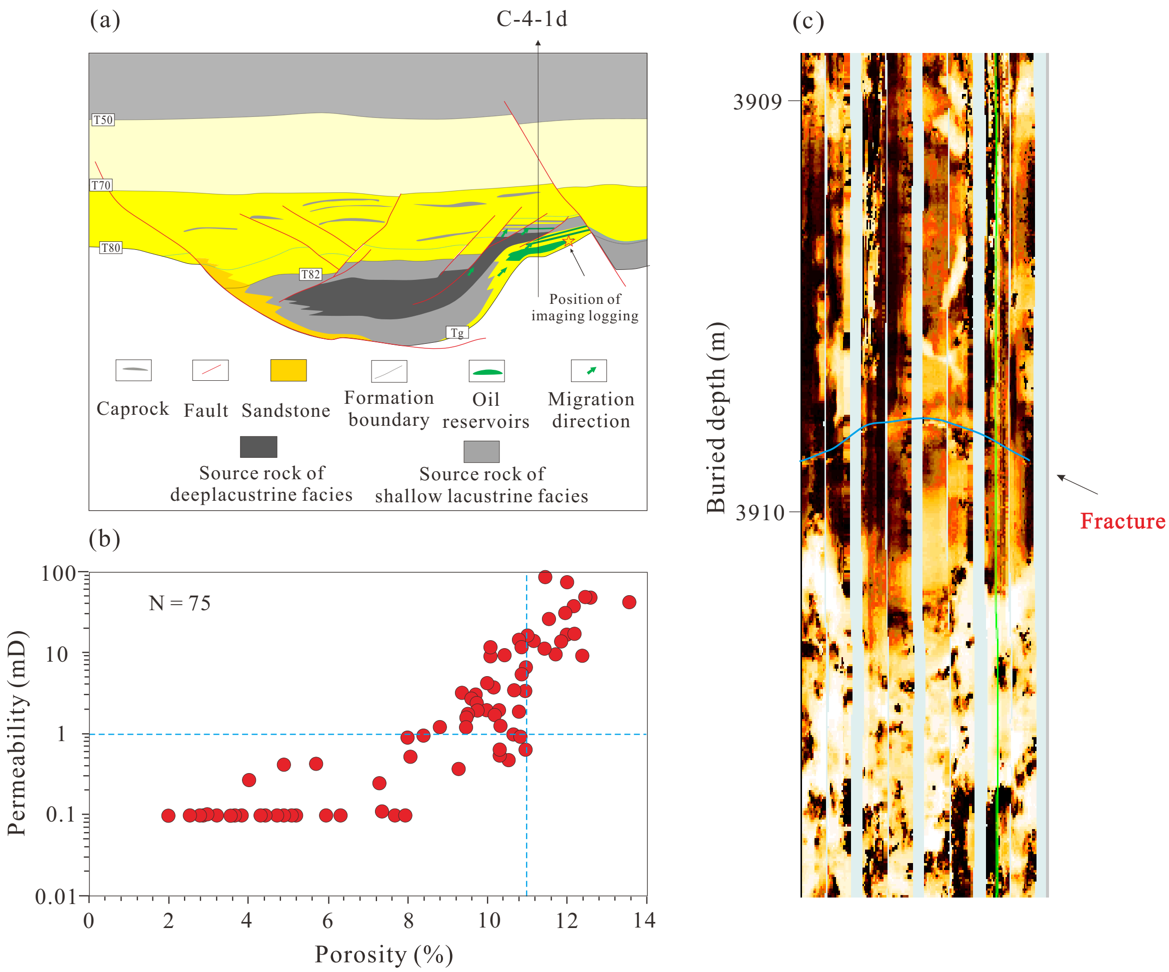

Fig. 9. (a) Diagram of forming model for WC_{4+5+6} oil and gas accumulations drilled by C-4-1d well; (b) Intersection diagram of reservoir porosity and permeability of C-4-1d WC_{4+5+6} reservoir; (c) Image-log map of WC_{4+5+6} reservoir in C-4-1d well.

reservoir characteristics, it can be inferred that WC_{1+2+3} oil and gas accumulation drilled by the B-1s-1d well is formed by hydrocarbon injected into the tight reservoir (Guo et al., 2017).

4.3.3 Characteristics of reformed oil and gas accumulations in C-HDF

The WC_{4+5+6} oil and gas accumulation drilled by the C-4-1d well is located in the southern edge of LF13s, which also is distributed in C-HDF (Figs. 1(a) and (b)). This accumulation is a lithological reservoir and also a typical reformed hydrocarbon accumulation reservoir in C-HDF. It is located in a structure where many faults are developed and the thick mudstone layer of WC_3 and WC_4 provide an excellent sealing condition (Fig. 9). The porosity of this oil and gas accumulation is lower than that corresponding to BHAD, which mainly ranges from 7.8% to 12%. However, the permeability of this oil and gas accumulation is higher than that corresponding to BHAD, which mainly ranges from 1 to 100 mD (Fig. 9(b)). This may be due to the fact that the reservoir was reformed by densely developed faults. The fault will create dense fracture zones in the surrounding rock near the fracture section, which will significantly improve the permeability of the reservoir (Fu et al., 2015). Image-log data show obvious fracture development traces in the WC reservoir in the C-4-1d well (Fig. 9(c)), which further supports the hypothesis that the reservoir has been reformed by fractures. Due to the effect of fracture reformation, the WC_{4+5+6} oil and gas accumulation drilled by the C-4-1d well has high hydrocarbon production despite its low porosity, and it is also an important commercial oil flow producing reservoir in the Lufeng Depression. Dai et al. (2019) reported that the main hydrocarbon charging period of the WC reservoir in Lufeng Depression is about 12 Ma. During this time, the deep of WC reservoir in C-4 well block did not exceed the BHAD. It can be determined that the WC_{4+5+6} oil and gas accumulation drilled by the C-4-1d well was conventional oil and gas accumulation in this period, and the reservoir gradually evolves into a tight reservoir with the increase of burial depth. Thus, this reservoir has some features of conventional oil and gas accumulations: Its source rock is separated from the reservoir, and oil and gas migrate over a short distance through sandstone (Fig. 9).

5. Discussion

Restricted by the actual conditions of offshore exploration and development, it is difficult to reconstruct the Paleogene

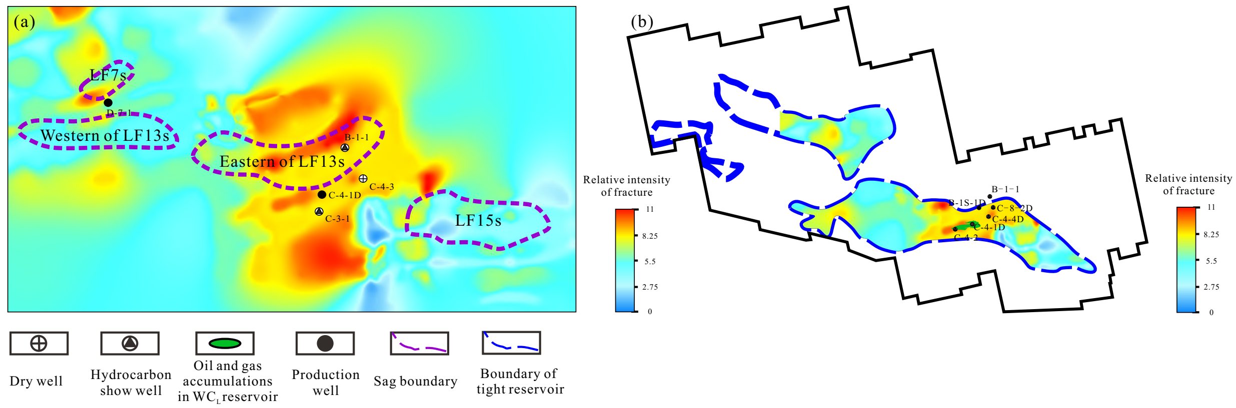

Fig. 10. (a) Relative intensity of fracture in WC_{4+5+6} of Lufeng sag; (b) Overlap diagram of relative intensity of fracture and tight reservoir range in WC_{4+5+6} of Lufeng sag.

reservoirs in the Lufeng Depression. In addition, offshore oil and gas exploration and development has mainly focused on commercial reservoirs in recent years (Tian et al., 2019). Therefore, for the practical exploration of Paleogene reservoir, the focus within F-HDF should be conventional oil and gas reservoirs, which should be found at high points of the trap. In C-HDF, the reformed hydrocarbon accumulation reservoir should be regarded as the main exploration object, which should be found in areas with many fractures. However, the unreformed reservoirs in C-HDF should not be focused on at the present stage, but only once the offshore artificial reservoir technology has matured. For the Lufeng Depression, the exploration idea of conventional oil and gas reservoirs in F-HDF is already mature, while the exploration level of reformed hydrocarbon accumulation reservoir in C-HDF is low. Thus, to determine the future exploration direction of WC_{4+5+6} reservoir, it is necessary to accurately predict the distribution of reformed reservoir. In this paper, the finite element numerical simulation software ANSYS was used to simulate the paleo-tectonic stress field formed by structural fractures in the study area, and the density of fractures in the WC_{4+5+6} was quantitatively predicted (Fig. 10(a)). The results show that fractures are well developed in LF13s, and the fracture density is large, which has a significant effect on the tight reservoir. The WC_{4+5+6} oil and gas accumulations drilled by the C-4-1d well are located in the tight reservoir area where fractures are the most developed (Fig. 10(b)). According to the overlap diagram of the relative intensity of fracture and tight reservoir range in WC_{4+5+6}, high fracture density is found in the C-4 well block, C-8 well block and the western part of C-8 well block in LF13s, which is the development area of reformed reservoir and has a good exploration prospect (Fig. 10(b)).

6. Conclusions

1) The buried depth corresponding to BHAD in the Lufeng Depression ranges from 3,500 to 4,000 m, which becomes gradually shallower from the interior to the edge of the depression. The HADL in the Lufeng sag is about 5,800 m.
2) In the Lufeng Depression, the whole EP_{1+2} reservoir is distributed within F-HDF, and most of the EP_{3+4} and WC_{1+2+3} reservoirs are also in F-HDF. Meanwhile, most of the WC_{4+5+6} reservoir and a limited part of WC_{1+2+3} reservoir exceed BHAD and are in C-HDF. In addition, the WC_{4+5+6} oil and gas accumulation drilled by the C-4-1d well is an important reformed oil and gas accumulation in C-HDF.
3) In the Lufeng Depression, the exploration focus of Paleogene oil and gas should be on conventional oil and gas reservoirs in F-HDF and reformed oil and gas accumulations in C-HDF. For the EP and WC_{1+2+3} reservoirs, conventional oil and gas reservoir exploration should be focused on, and the tight reservoir of WC_{4+5+6} should be explored in the high fracture density area in C-4 and C-8 well blocks and the west of C-8 well block.

Acknowledgement

This study was supported by the Major National R&D Projects of China (Grant No. 2016ZX05024-004) and the research project of CNOOC (Shenzhen) (Grant No. SCKY-2020-SZ-21).

Conflict of interest

The authors declare no competing interest.

References

Almedallah, M., Altaheini, S. K., Clark, S., et al. Combined stochastic and discrete simulation to optimise the economics of mixed single-horizontal and multilateral well offshore oil developments. Petroleum Exploration and Development, 2021, 48(5): 1183-1197.

Dai, Y., Niu, Z., Wang, D., et al. Differences of hydrocarbon enrichment regularities and their main controlling factors between Paleogene and Neogene in Lufeng sag, Pearl River Mouuth Basin. Acta Petrolei Sinica, 2019, 40(s1):

41-52. (in Chinese)
Esmaili, S., Mohaghegh, S. D. Full field reservoir modeling of shale assets using advanced data-driven analytics. Geoscience Frontiers, 2016, 7(1): 11-20
Fu, X., Jia, R., Wang, H., et al. Quantitative evaluation of fault-caprock sealing capacity: A case from Dabei-Kelasu structural belt in Kuqa Depression, Tarim Basin, NW China. Petroleum Exploration and Development, 2015, 42(3): 329-338.
Ge, J., Zhu, X., Zhao, X., et al. Tectono-sedimentary signature of the second rift phase in multiphase rifts: A case study in the Lufeng Depression (38-33.9 Ma), Pearl River Mouth Basin, south China sea. Marine and Petroleum Geology, 2020, 114: 104218.
Guo, Y., Pang, X., Li, Z., et al. The critical buoyancy threshold for tight sandstone gas entrapment: Physical simulation, interpretation, and implications to the Upper Paleozoic Ordos Basin. Journal of Petroleum Science and Engineering, 2017, 149: 88-97.
Jia, C., Pang, X., Yan, S. The mechanism of unconventional hydrocarbon formation: Hydrocarbon self-sealing and intermolecular forces. Petroleum Exploration and Development, 2021, 48(3): 507-526.
Karlsen, D. A., Skeie, J. E. Petroleum migration, faults and overpressure, part I: Calibrating basin modelling using petroleum in traps—a review. Journal of Petroleum Geology, 2006, 29(3): 227-256.
Liu, Z. Differences and influencing factors of the buoyance controlling reservoir limitation in different zones of Nanpu Sag. Beijing, China University of Petroleum (Beijing), 2018. (in Chinese)
Magoon, L. B., Dow, W. G. The petroleum system, in Fractals in the The Petroleum System—From Source to Trap, edited by L. B. Magoon and W. G. Dow, American Association of Petroleum Geologists, Tulsa, pp. 3-24, 1994.
Niu, Z., Liu, G., Ge, J., et al. Geochemical characteristics and depositional environment of Paleogene lacustrine source rocks in the Lufeng Sag, Pearl River Mouth basin, South China Sea. Journal of Asian Earth Sciences, 2019, 171: 60-77.
Pang, X., Hu, T., Larter, S., et al. Hydrocarbon accumulation depth limit and implications for potential resources prediction. Gondwana Research, 2022, 103: 389-400.
Pang, X., Jia, C., Chen, J., et al. A unified model for the formation and distribution of both conventional and unconventional hydrocarbon reservoirs. Geoscience Frontiers, 2021a, 12(2): 395–711.
Pang X., Jia, C., Wang, W., et al. Buoyance-driven hydrocarbon accumulation depth and its implication for unconventional resource prediction. Geoscience Frontiers, 2021b, 12(4): 101133.
Shanley, K. W., Cluff, R. M., Robinson, J. W. Factors controlling prolific gas production from low-permeability sandstone reservoirs: Implications for resource assessment, prospect development, and risk analysis. AAPG Bulletin, 2004, 88(8): 1083-1121.
Shi, D., Li, M., Pang, X., et al. Fault-fracture mesh petroleum plays in the Zhanhua Depression, Bohai Bay Basin: Part 2. Oil-source correlation and secondary migration mechanisms. Organic Geochemistry, 2005, 36(2): 203-223.
Smith, M. G., Bustin, R. M. Late Devonian and Early Mississippian Bakken and Exshaw black shale source rocks, Western Canada Sedimentary Basin: a sequence stratigraphic interpretation. AAPG Bulletin, 2000, 84(7): 940-960.
Tan, Z., Wang, W., Li, W., et al. Controlling factors and physical property cutoffs of the tight reservoir in the Liuhe Basin. Advance in Geo-Energy Research, 2017, 1(3): 190-202.
Tian, D., Jiang, T., Liu, B., et al. Early Miocene sedimentary processes and their hydrocarbon implications in the Baiyun Sag of Pearl River Mouth Basin, northern South China sea. Marine and Petroleum Geology, 2019, 101: 132-147.
Wang, C., Sun, Y. Development of Paleogene depressions and deposition of lacustrine source rocks in the Pearl River Mouth Basin, northern margin of the South China Sea. AAPG Bulletin, 1994, 78(11): 1711-1728.
Wang, M., Wilkins, R. W. T., Song, G., et al. Geochemical and geological characteristics of the Es3L lacustrine shale in the Bonan sag, Bohai Bay Basin, China. International Journal of Coal Geology, 2015, 138: 16-29
Wang, W., Pang, X., Chen, Z., et al. Improved methods for determining effective sandstone reservoirs and evaluating hydrocarbon enrichment in petroliferous basins. Applied Energy, 2020, 261: 114457.
Wang, W., Zheng, D., Sheng, G., et al. A review of stimulated reservoir volume characterization for multiple fractured horizontal well in unconventional reservoirs. Advance in Geo-Energy Research, 2017, 1(1): 54-63.
Wang, X., Zhang, X., Lin, H., et al. Paleogene geological framework and tectonic evolution of the central anticlinal zone in Lufeng 13 sag, Pearl River Mouth Basin. Petroleum Research, 2019, 4(3): 238-249.
Wu, S., Liu, J., Xu, H., et al. Application of frequency division inversion in the prediction of heterogeneous natural gas hydrates reservoirs in the Shenhu Area, South China Sea. China Geology, 2022, 5(2): 251-266.
Xie, Z., Wei, J., Zheng, J., et al. A 3D basin modeling study of the factors controlling gas hydrate accumulation in the Shenhu Area of the South China Sea. China Geology, 2022, 5(2): 218-233.
Yuan, J., Jiang, R., Zhang, W., et al. The workflow to analyze hydraulic fracture effect on hydraulic fractured horizontal well production in composite formation system. Advance in Geo-Energy Research, 2018, 2(3): 319-342
Zhang, S., Liang, D., Gong, Z., et al. Geochemistry of petroleum systems in the eastern Pearl River Mouth Basin: Evidence for mixed oils. Organic Geochemistry, 2003, 34(7): 971-991.
Zou, C., Zhang, G., Yang, Z., et al. Geological concepts, characteristics, resource potential and key techniques of unconventional hydrocarbon: on unconventional petroleum geology. Petroleum Exploration and Development, 2013, 40(4): 385-399.